Project 6 - Detection of resonances for the modelling of resonant tunneling devices

S. Baltieri, A. Carballosa, M. Feder, A. Tonini, M. Zarcheva

August 29, 2019

Contents

1   Introduction

In Quantum mechanics, the simplest unidimensional problems are the cases for a potential form
of a barrier and a well, illustrated in Figure 1. For each one of these problems, one unique
phenomenon occurs that is only observed in the quantum realm. In the first case, when one particle
faces a potential barrier with energy lower than the height of the barrier, in the classical point of
view, the particle will be reflected assuming that the impact with the barrier preserves energy and
momentum. However, in quantum mechanics, the particle has a non-zero probability to appear
on the other side of the barrier, since the particle does not have now a deterministic trajectory,
but a density of probability of being at position x and time t distributed across a determined
region of space. This density of probability can be obtained through the Schröedinger equation
introducing the appropriate initial and boundary conditions to account for the potential. In this
sense, the particles propagates in space according to a wave function φ, and when encountering
the barrier will have a probability of being reflected and a probability of being transmitted. The
latter is measured through the transmission coefficient.

<div align="center">(a)   (b)</div>
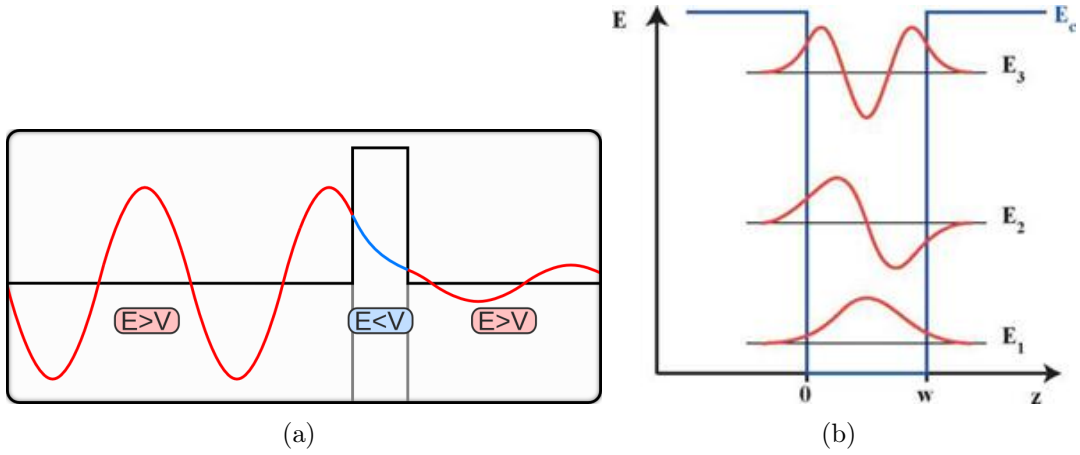
Figure 1: Quantum tunneling through a potential barrier (fig a)) and a potential well with
its discrete energy levels (fig b)). Figures extracted from http://elektroarsenal.net/
quantum-wells.html and https://brilliant.org/wiki/quantum-tunneling/

In the problem of one particle enclosed in the quantum well, by solving Schröedinger equation
one finds that the energy states of the particle are discretized as Figure 1 shows, instead of the
continuous range that one would expect in classical dynamics.

Now, here what concerns us is the interesting problem of putting together two or more potential
barriers creating a quantum well in the middle. This is what occurs in the resonant tunneling
devices, which receive its name because it is observed that for some incident energy of the electrons
the transmission coefficient equals the unity. This is, the electrons go through the device without
"seeing" the barriers. The nature of this curious effect arises from the discretization of the energy
states inside the quantum well, producing that when the energy of the incident electron coincides
with one of the energy levels of the well, the transmission coefficient peaks to one, as shown
in Figure 2. This effect allows for an application of resonant tunneling transistors as promising
switching devices, ideal for memory storing.

In this work, we attempt to study the problem of two or more potential barriers from a numerical
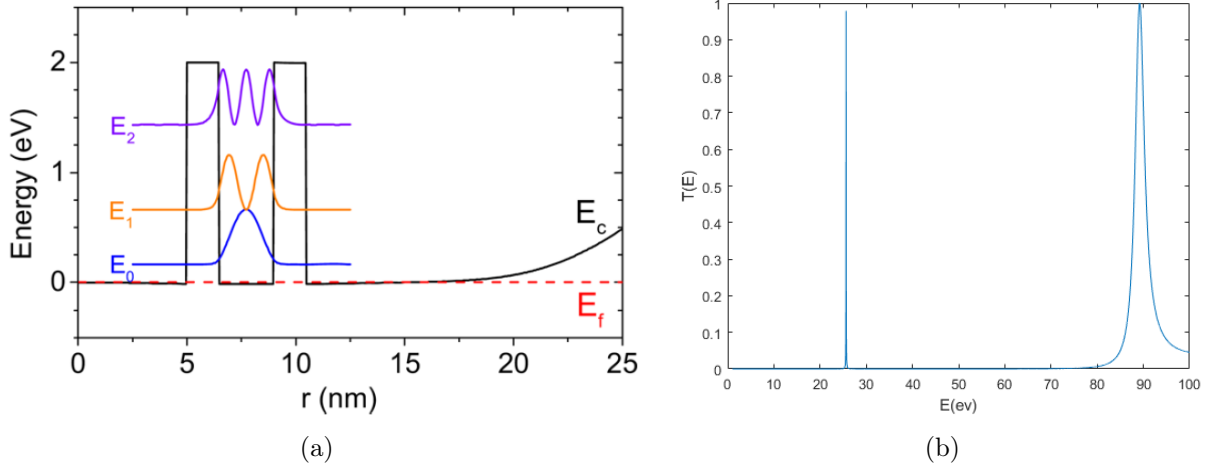
Figure 2: Resonant tunneling (fig a)) and transmission coefficient (fig b)) for a double barrier. Fig. a) was extracted from http://dx.doi.org/10.1063/1.3701586

point of view and in an ideal situation (with null potential difference between the extremities of the device). For this purpose, we find that the main feature of the problem is to characterize accurately the transmission coefficient in function of the incident energy, since this curve will provide all the information needed on the energy resonances and the transmission peaks. Considering that each value of the energy will imply solving one time the Schröedinger equation, we must also find a strong optimization to the numerical implementation in order to reduce the computational work, solving therefore a more reasonable number of differential equations. The optimization that we will describe here will be that of an adaptive mesh scheme in the energy discretization.

2 Preliminary computations

2.1 Finding the transmission coefficient T

As a beginning, we will make a quick review of the process of *quantum tunneling*.

Let us consider a current or voltage wave, travelling through a transmission line from a generating source towards a load. This wave becomes an *incident wave* when it meets a discontinuity or another medium with different propagation characteristics. In this situation, some or all of the wave will be reflected back in the direction of the origin [1].

If a wave travelling within a force field reaches a region that has a potential, significantly higher than the potential at the points surrounding it, we observe an incident wave upon a *potential barrier*. According to the laws of classical mechanics, a particle needs to have a potential energy, higher than the energy of the barrier, in order to be able passing through it. If that is not the case, the particle should be reflected in the opposite direction. However, on quantum level (observing particles and energies on subatomic scale), it is possible for a particle to pass trough the barrier, without having the potential energy required. This phenomenon is known as *quantum tunnelling*.

4

The quantity that describes the probability of a particle tunneling through a barrier is the so called *transmission coefficient*. By definition, the *transmission coefficient* T is described by the following ratio:

$$T = \frac{J_{trans}.\overline{n}}{J_{inj}.\overline{n}},$$

where J_{inj} is the *probability current* in the wave incident upon the barrier with normal unit vector $\overline{n}$, and J_{trans} is the *probability current* in the wave that has passed on the other side of the barrier [2].

In the following section, we will introduce the concept of *probability current*.

2.2 The probability current

Probability current (probability flux) is a formalism in quantum mechanics that describes the flow of probability. It is defined as the probability per unit time, per unit area. We need to establish a connection between the variables in the model and the unknown probability flux in order to compute the transmission coefficient T.

It is not a coincidence that the quantity of interest is called probability *flux*. When talking about flux, the first thing to come in mind is the continuity equation. It appears that there is a conserved quantity in the process, that is, the *probability density* and we can obtain the definition of probability flux, using it [3]. If one thinks about the *probability density* as a heterogeneous fluid, then the *probability current* is the rate of flow of this fluid [4].
The *probability density* is defined as

$$P(x,t) = |\psi|^2 = \psi^*(x,t)\psi(x,t),$$

where ψ^* is the complex conjugate of ψ.

Differentiating it with respect to time, we obtain

$$\frac{\partial}{\partial t}P(x,t) = \left[\frac{\partial \psi^*}{\partial t}\psi + \psi^*\frac{\partial \psi}{\partial t}\right]. \tag{1}$$

Using the *Shrödinger* equaiton for ψ and its complex conjugate, multiplying them for ψ^* and ψ respectively, and replacing them in (1), we arrive at

$$\psi^*\left(\mathbf{i}\hbar\frac{\partial \psi}{\partial t}\right) = \left(-\frac{\hbar^2}{2m}\frac{\partial^2 \psi}{\partial x^2} + V(x)\psi\right)\psi^*$$

$$\psi\left(-\mathbf{i}\hbar\frac{\partial \psi^*}{\partial t}\right) = \left(-\frac{\hbar^2}{2m}\frac{\partial^2 \psi^*}{\partial x^2} + V(x)\psi^*\right)\psi$$

$$\frac{\partial}{\partial t}P(x,t) = \frac{1}{\mathbf{i}\hbar}\left[\frac{\hbar^2}{2m}\frac{\partial^2\psi^*}{\partial x^2}\psi - \cancel{V(x)\psi^*\psi} - \frac{\hbar^2}{2m}\frac{\partial^2\psi}{\partial x^2}\psi^* + \cancel{V(x)\psi^*\psi}\right]$$
$$= \frac{\hbar}{2m\mathbf{i}}\frac{\partial}{\partial x}\left[\frac{\partial\psi^*}{\partial x}\psi - \psi^*\frac{\partial\psi}{\partial x}\right].$$

We define $j(x,t)$ as the *the probability current*:

$$j(x,t) = \frac{\hbar}{2m\mathbf{i}}\left[\psi^*\frac{\partial\psi}{\partial x} - \frac{\partial\psi^*}{\partial x}\psi\right] = \frac{\hbar}{m}Im\left(\psi^*\frac{\partial\psi}{\partial x}\right). \tag{2}$$

We have just derived the probability conservation equation

$$\frac{\partial P(x,t)}{\partial t} + \frac{\partial j(x,t)}{\partial x} = 0. \tag{3}$$

,

Now, we can use (2) to compute the transmission coefficient.

2.3 Time-independent formulation

The time-dependent *Shrödinger* equation predicts that wave functions can form stationary states, called standing waves. In physics, a standing wave (stationary wave) is a wave which oscillates in time but whose peak amplitude profile does not move in space. The peak amplitude of the wave oscillations at any point in space is constant with time. This phenomenon usually occurs as a result of interference between two waves traveling in opposite directions, for example in the case of resonance [5].

Such stationary state is an eigenvector of the Hamiltonian. This means, that we are observing a situation where the system has a single definite energy (instead of a quantum superposition of different energies). It is also called *energy eigenvector*.

For a single-particle Hamiltonian, a stationary state means that the particle has a constant probability distribution for its position, its velocity, its spin, etc. (this is true assuming that the Hamiltonian is unchanging in time). We should note that the wavefunction itself is not stationary [5].

These states are particularly important as their individual study later simplifies the task of solving the time-dependent *Shrödinger* equation for any state. Stationary states can be described by the time-independent *Shrödinger* equation.

The time-independent formulation can be obtained, using the classical method of separation of variables, as following.

Let

$$\psi(x,t) = \varphi(x)f(t)$$

$$\mathbf{i}\hbar\varphi(x)\frac{df(t)}{dt} = -\frac{\hbar^2}{2m}\frac{d^2\varphi(x)}{dx^2}f(t) + V(x)\varphi(x)f(t)/\cdot\frac{1}{\varphi(x)f(t)}$$

$$\frac{1}{f(t)}\mathbf{i}\hbar\frac{df(t)}{dt} = -\frac{\hbar^2}{2m}\frac{1}{\varphi(x)}\frac{d^2\varphi(x)}{dx^2} + V(x) = const. = E.$$

Multiplying by $\varphi(x)$ the space equation

$$-\frac{\hbar^2}{2m}\frac{d^2\varphi(x)}{dx^2} = (E - V(x))\varphi(x), \tag{4}$$

where E is a constant equal to the energy level of the system.

2.4 Nondimesionalization

Before we start with the numerical computations, what we can notice, is that some very small numbers appear in the main equation. (2.4)

$$\frac{\hbar^2}{m} = \frac{(1.054571726 \cdot 10^{-34}Js)^2}{9.109383702 \cdot 10^{-31}kg} \approx 1.220852652 \cdot 10^{-38}\frac{J^2s^2}{kg} \approx 4.756006764 \cdot 10^{-1}\frac{eV^2s^2}{kg}$$
$$1eV = 1.602176634 \cdot 10^{-19}J$$

In order to avoid computations with such small numbers, we shall derive a non-dimensional form of the model. For this purpose, we use the following change of variables:

$$\overline{x} = \frac{x}{\lambda} \qquad \widetilde{V} = \frac{V(\overline{x})}{E_c} \qquad \widetilde{E} = \frac{E(\overline{x})}{E_c}$$

$$E_c := \frac{\hbar^2}{m\lambda^2} \qquad [E_c] = ML^{-2}T^{-2},$$

with λ-characteristic length, which is usually set to be the length of the domain of interest, and E_c the characteristic energy.
Making a substitution in (4), we obtain

$$\frac{1}{2}\frac{d^2\varphi}{d\overline{x}^2} = (\widetilde{V}(\overline{x}) - \widetilde{E})\varphi(\overline{x}) \tag{5}$$

From now on, all the experiments in the report are derived using (5).

3 A finite difference approximation for Schrödinger equation

3.1 Finite differences method

Consider the problem of approximating the derivative of a function f in an interval $[a,b]$. A natural way to proceed is to introduce N nodes in $[a,b]$ $x_k, k=1,\ldots,N$ with $x_1 = a$, $x_n = b$ and $x_{k+1} = x_k + h, k = 1,\ldots,N-1$, where $h = \frac{b-a}{N-1}$. Fixed x_i, we approximate $f'(x_i)$ with he value of the node $f(x_k)$ in the following way:

$$h \sum_{k=-m}^{m} \alpha_k u_{i-k} = \sum_{k=-m}^{m} \beta_k f(x_{i-k}), \tag{6}$$

where $\{\alpha_k\}_{k=-m}^{k=m}, \{\beta_k\}_{k=-m}^{k=m} \subseteq \mathbb{R}$. We note that after setting the coefficients $\{\alpha_i\}$ and $\{\beta_i\}$, to determine the values u_i, with $i \in \{0,\ldots,n\}$, it is necessary to solve a linear system.

In the case of classical finite differences, the intrinsic definition of derivative is used:

$$f'(x_i) = \lim_{h\to 0^+} \frac{f(x_i + h) - f(x_i)}{h}. \tag{7}$$

By replacing the limit operation with the incremental relationship with h finite, we get the following approximation:

$$u_i = \frac{f(x_{i+1}) - f(x_{i-1})}{2h}, \quad 2 \leq i \leq N-1. \tag{8}$$

The second member of (8) is called *finite difference centered* and corresponds geometrically to have replaced a $f'(x_i)$ with the angular coefficient of the line passing through the points $(x_{i-1}, f(x_i))$ e $(x_i, f(x_{i+1}))$. Using Taylor series development, we get

$$f'(x_i) - u_i = -\frac{h^2}{6} f'''(\xi_i). \tag{9}$$

Than (8) is an approximation of second order with respect to h.

3.2 For Schrödinger equation

We discretize our domain $\Omega = (a,b)$ with N points and the uniform mesh is made by $N-1$ intervals of length $h = \frac{b-a}{N-1}$.

For the sake of simplicity we consider the nondimensional time independent equation with *transparent boundary conditions*, in $\Omega = (0,1)$, namely

$$\varphi''(x) + 2(E - V(x))\varphi(x) = 0$$

and conditions

$$\mathbf{i}k\varphi(0) + \varphi'(0) = 2\mathbf{i}k,$$

$$\varphi'(1) = \mathbf{i}k_2\varphi(1),$$

where $\mathbf{i}$ is the imaginary unit and $k_2 = \sqrt{k^2 + 2(V(0) - V(1))}$, $k = \sqrt{2(E - V(0))}$.

Here $V : \mathbb{R} \to \mathbb{R}$ is the potential, which can be assumed to be piecewise constant. With the centered, second order, finite difference approach, the discretized equation becomes

$$\frac{\varphi_{i+1} - 2\varphi_i + \varphi_{i-1}}{h^2} + 2(E - V(x_i))\varphi_i = 0, \quad i = 1, \ldots, N.$$

We can easily re-write the equation as a linear system using the fact that the part corresponding to the second derivative can be written as a *matrix-vector* product $A \cdot \boldsymbol{\varphi}$, where

$$A = \frac{1}{h^2} \begin{bmatrix} -2 & 1 & 0 & 0 & \ldots & 0 \\ 1 & -2 & 1 & 0 & \ldots & 0 \\ 0 & \ddots & \ddots & \ddots & \ddots & \vdots \\ \vdots & \ddots & \ddots & \ddots & \ddots & 0 \\ 0 & \ldots & 0 & 1 & -2 & 1 \\ 0 & \ldots & 0 & 0 & 1 & -2 \end{bmatrix}$$

and the boundary conditions has still to be imposed. The above tridiagonal matrix can be easily generated with the following MatLab command:

```
A=toeplitz(sparse([1,1],[1,2],[-2,1]/(h^2),1,m))
```

Looking at the other term of the equation, one can easily see that the whole equation becomes

$$(A + B)\boldsymbol{\varphi} = \mathbf{0},$$

where $(B)_{i,j} = 2(E - V(x_i))\delta_i^j$.

3.3 Boundary conditions

We write the first boundary condition by discretizing the first derivative with a second order approximation, by introducing a *ghost node* (or virtual node) $x_0 = x_1 - h$

$$\mathbf{i}k\varphi_1 + \frac{\varphi_2 - \varphi_0}{2h} = 2\mathbf{i}k.$$

Now, we compute φ_0 as a function of φ_1, φ_2, and we put it into the first line of the discretized system, which is

$$\frac{\varphi_2 - 2\varphi_1 + \varphi_0}{h^2} + 2(E - V(x_1))\varphi_1 = 0.$$

This leads to the following first line:

$$\varphi_1\left(\frac{2\mathbf{i}k}{h} - \frac{2}{h^2} + 2(E - V(x_1))\right) + \frac{2}{h^2}\varphi_2 = \frac{4\mathbf{i}k}{h}.$$

This strategy preserves the second order of the numerical scheme. The very same argument applies to the other boundary condition. After these conditions we will end up with a RHS $\boldsymbol{b}$ which is zero everywhere except for the first component $\boldsymbol{b}(1) = \frac{4\mathbf{i}k}{h}$.

Finally, the linear system to solve is

$$\frac{1}{h^2}\begin{bmatrix} 2\mathbf{i}hk - 2 + 2h^2(E - V(x_1)) & 2 & 0 & 0 & \cdots & & 0 \\ 1 & -2 & 1 & 0 & \cdots & & 0 \\ 0 & \ddots & \ddots & \ddots & \ddots & & \vdots \\ \vdots & \ddots & \ddots & \ddots & \ddots & & 0 \\ 0 & \cdots & 0 & 1 & -2 & & 1 \\ 0 & \cdots & 0 & 0 & 2 & 2\mathbf{i}hk_2 - 2 + 2h^2(E - V(x_m)) \end{bmatrix} \cdot \begin{bmatrix} u_1 \\ u_2 \\ \vdots \\ \vdots \\ u_{m-1} \\ u_m \end{bmatrix} = \begin{bmatrix} \frac{4\mathbf{i}k}{h} \\ 0 \\ \vdots \\ \vdots \\ \vdots \\ 0 \end{bmatrix}.$$

It's solved by using the default command *backslash* in MatLab, which can easily handle complex arithmetic.

4   Consistency of the scheme

In order to show the consistency of the scheme, we insert the analytical solution $\varphi(x)$ in the numerical scheme

$$\frac{\varphi(x_{i+1}) - 2\varphi(x_i) + \varphi(x_{i-1})}{h^2} + 2(E - V(x_i)) = 0 \quad i = 2, \ldots, N - 1$$

and, assuming $\varphi \in C^4$, we expand in Taylor series about $x = x_i$

$$\varphi''(x_i) + 2(E - V(x_i)) + \varphi^{(4)}(\xi)\frac{h^2}{12} + \mathcal{O}(h^4), \quad \xi \in (x_{i-1}, x_i).$$

Since $\varphi(x)$ is the analytical solution, what remains is just $\varphi^{(4)}(\xi)\frac{h^2}{12} + \mathcal{O}(h^4), \quad \xi \in (x_{i-1}, x_i).$

5 Stability

6 Order of convergence

In order to show numerically the order of convergence, we compared the infinity norm of the difference between the analytical solution and the numerical one for a different number of grid points. The constants in the analytical solution has been computed by solving a linear system. As a potential we chose $V(x) = 50$, $x \in (0,1)$. In Figure 3 the following logarithmic scaled plot we can appreciate the right order of convergence.
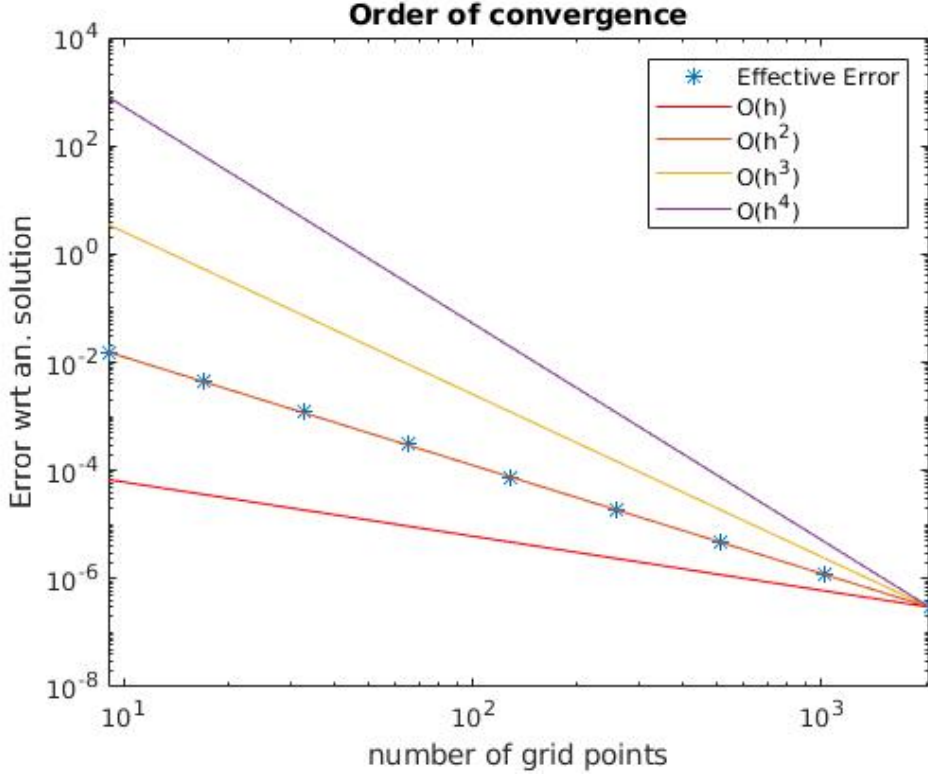

Figure 3: Order of convergence depending on the number of grid points

7 Implementation

Now we describe the code. First of all we set the constants, the potential and the space interval. We need to find the energy levels where the resonance is. We will use a space uniform mesh to approximate the probability density function for fixed level of energy using the method described previously after the nondimensionalization. We set an energy uniform mesh, we find the approximate solutions for the different energy levels and we compute the transmission coefficients for these energy values, then we refine uniformly the mesh used (e.g. dividing by 2 the length of the energy subintervals because we don't want to increase too much the computational cost) and we compute the new approximate solutions and transmission coefficients. Now we need to locate the energy regions where the resonance could be. We compare the transmission coefficients of the

actual energy mesh and the previous one. In the previous mesh we have less values of energy for which the transmission coefficient is computed, so we need more values for the previous transmission coefficients. We used a linear interpolation to compute the transmission coefficient for the missing values of energy. The transmission coefficient is a number between 0 and 1 therefore the difference of the transmission coefficients could be very small, so we computed the relative error between the logarithms. For every energy value of the current mesh when the relative error is greater than a fixed tolerance we store the energy point. These levels of energy identify the regions where we need to refine the energy mesh. We have to separate the regions to detect those where the error is too high and we need to refine the energy mesh and to avoid to refine the energy mesh where it is useless. We calculated the variation of the logarithm of the actual transmission coefficient and we studied it on the energy levels found previously. When we have a peak the variation before it is positive and then negative. The region of one peak is identified by the levels of energy where the variation first is positive (to find the part of the region on the left of the peak) and then is negative (to find the part of the region on the right of the peak). When the variation becomes positive from negative the region is over. For every region we compute the error on the logarithm of the transmission coefficient and, if it is greater than another fixed tolerance, we need to refine the energy mesh in that region (e.g. dividing by 5 or 10 the energy step). Now we have constructed a new mesh that becomes the current one and the one before the refinement becomes the previous one and we repeat this procedure until a maximum number of iteration is reached or the error is below a fixed tolerance.

In the next figures we will study the behavior of the transmission coefficient and the refinement of the energy mesh of two different potentials, one on the left side with two barriers and the other one on the right side with five barriers.

(a) 2 barriers potential
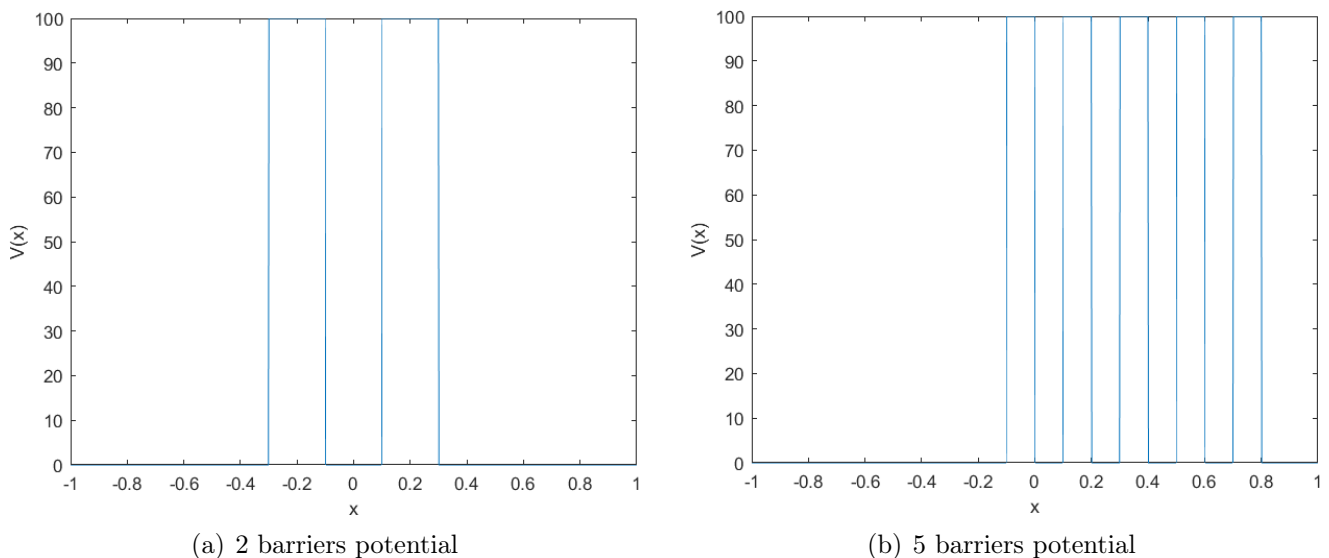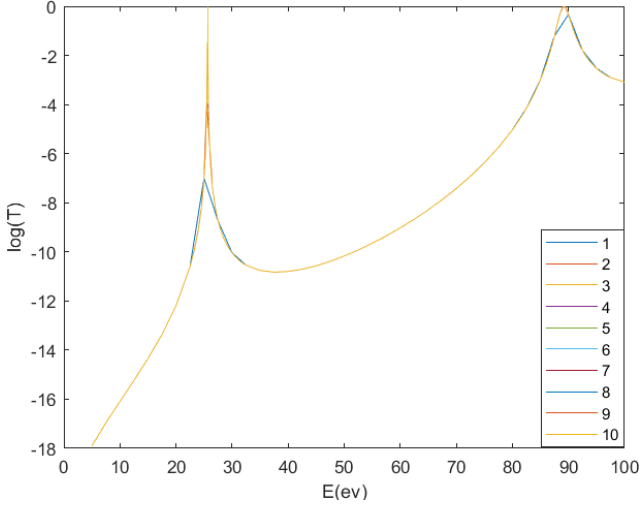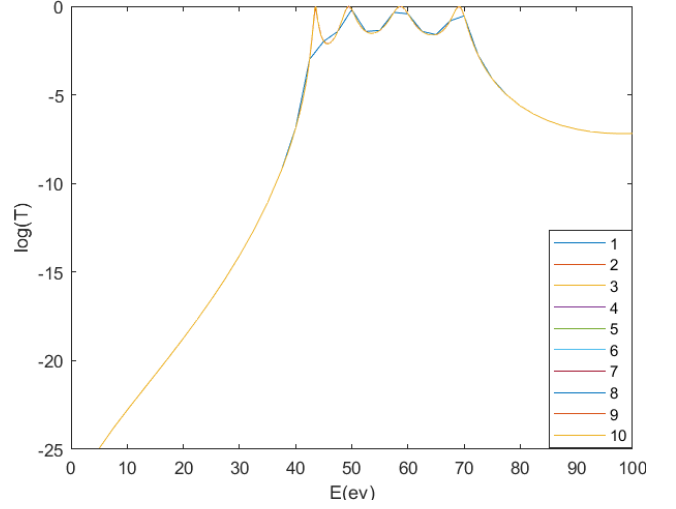
(b) 5 barriers potential

Figure 4: Potentials

In Figure 5 there are the approximations of the logarithm of the transmission coefficients after some iterations. We note that there are two peaks for the left potential and four for the right one. In Figure 6 there are the approximations of the transmission coefficients.

In Figure 7 we have on the left of the graphics the scale for the energy step represented with stars, on the right the scale for the transmission coefficient. We notice that near the peaks the energy step becomes really small.
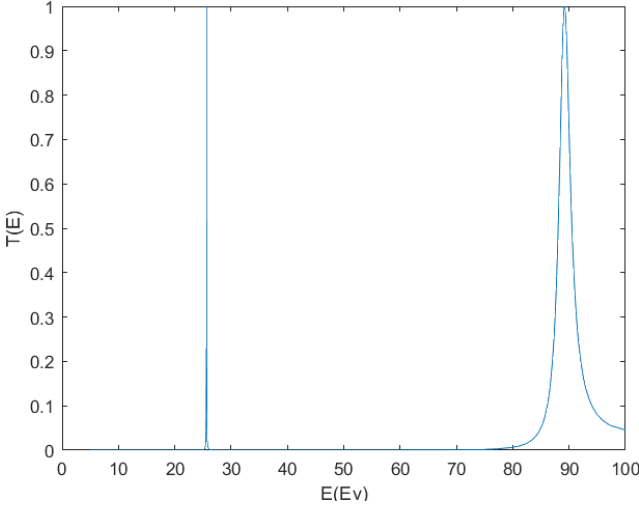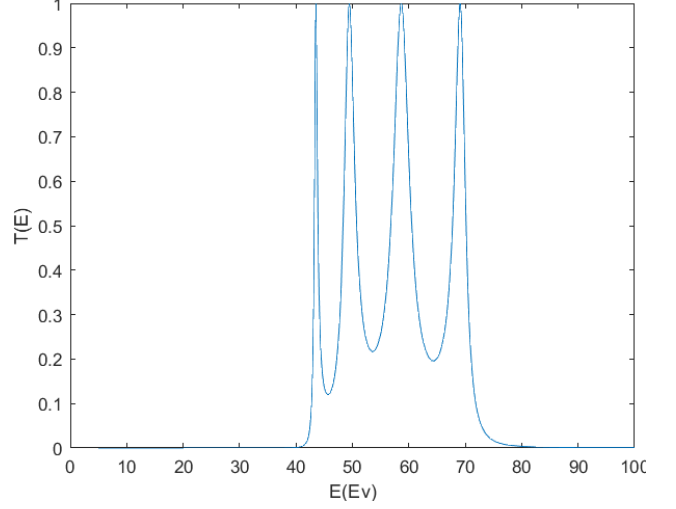
(a) 2 barriers potential

(b) 5 barriers potential

Figure 5: Approximations of the transmission coefficient at different iterations

(a) 2 barriers potential

(b) 5 barriers potential

Figure 6: Transmission coefficient

8 Possible improvement: Galerkin approach

Since the regularity of φ strongly depends on the regularity of the potential $V(x)$, with a finite difference approach one lose the second order approximation. Indeed, with piece-wise constant potential we have no more second order approximation. This observation leads to a Galerkin approach, requiring the solution $\varphi(x)$ to be less smooth than before.

Denoting with $H^1(0,1)$ the Sobolev space $W^{1,2}(0,1)$, as usual we take a $v \in H^1(0,1)$, multiply the equations by v and integrate by parts:

$$[\varphi'(x)v(x)]_0^1 - \int_0^1 \varphi'(x)v'(x)\mathrm{dx} + 2\int_0^1 (E - V(x))\varphi(x)v(x)\mathrm{dx} = 0, \quad v \in H^1(0,1)$$

13

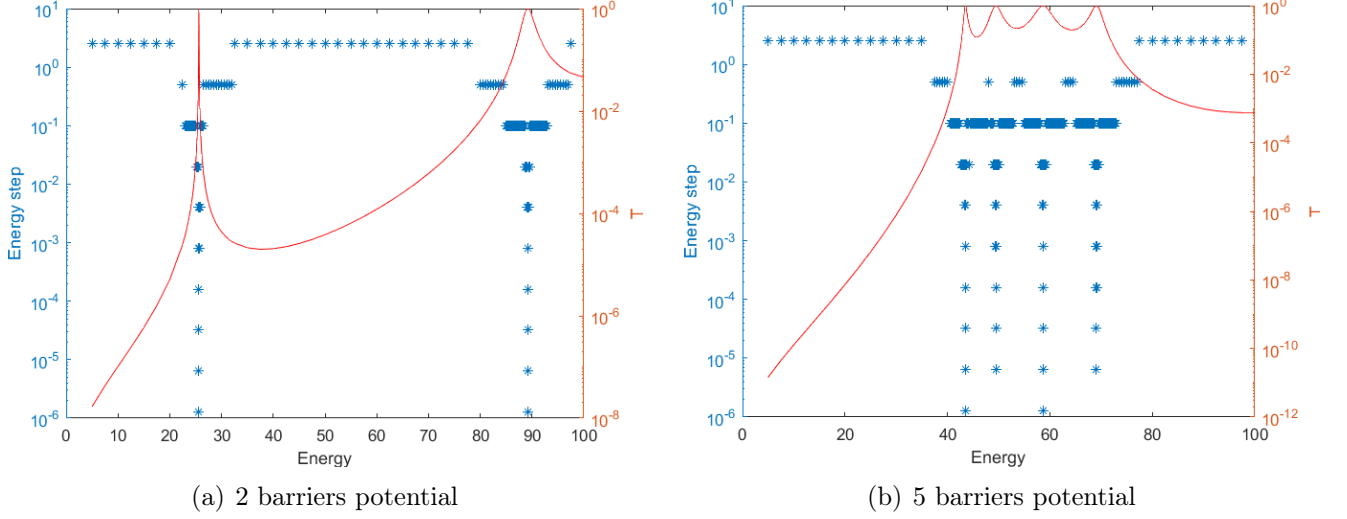(a) 2 barriers potential   (b) 5 barriers potential

Figure 7: Mesh refinement and transmission coefficient

Recalling that we have Robin boundary conditions, then in the weak formulation we will have terms proportional to φ. Using the fact that $\varphi'(0) = 2\mathbf{i}k - \mathbf{i}k\varphi(0)$ and $\varphi'(1) = \mathbf{i}k_2\varphi(1)$ then the weak formulation is to find $u \in H^1(0,1)$ such that the following identity:

$$\mathbf{i}k_2\varphi(1)v(1) + \mathbf{i}k\varphi(0)v(0) - 2\mathbf{i}k - \int_0^1 \varphi'v'\mathrm{dx} + 2\int_0^1 (E - V(x))\varphi v\mathrm{dx} = 2\mathbf{i}k, \quad (\star)$$

holds for every $v \in H^1(0,1)$.

In order to solve it, we restrict to a proper finite dimensional subspace X_h of H^1, made by piecewise linear functions, i.e. $X_h = \{w \in H^1(0,1) : w_{|[x_i,x_{i+1}]} \in \mathbb{P}([x_i, x_{i+1}])\}$. A basis of this space X_h is given by the "hat functions" $w(x)$ and therefore we have to search for $\varphi_h \in X_h$ such that $(\star)$ holds for every $v \in X_h$. In particular, we have

$$\varphi_h(x) = \sum_{i=1}^{N} (\varphi_h)_j w_j(x)$$

and the discrete problem is therefore to find $\varphi_h \in X_h$ s.t.

$$-\int_0^1 \sum_j (\varphi_h)_j w_j'(x) w_i'(x)\mathrm{dx} + 2\int_0^1 (E - V(x)) \sum_j (\varphi_h)_j w_j(x) w_i(x)\mathrm{dx} + \mathbf{i}k(\varphi_h)_1 w_1^2(0) + ik_2(\varphi_h)_N w_n^2(1) = 2\mathbf{i}k$$
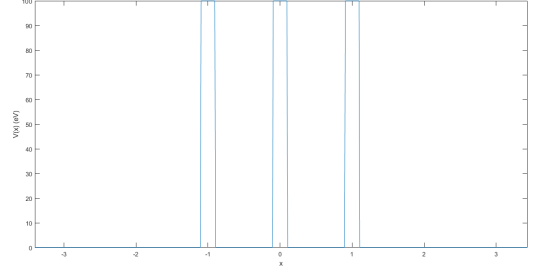
for $1 \le i \le N$

9 Validation

9.1 Variating the potential

Until now, we have tested identical potential barriers with the same value and ratio of width barrier/well. An important test now is to check if the optimization depends on the form of the potential. In Figure 8 we show the tested modified potentials and in Figure 9 and Figure 10 the results.
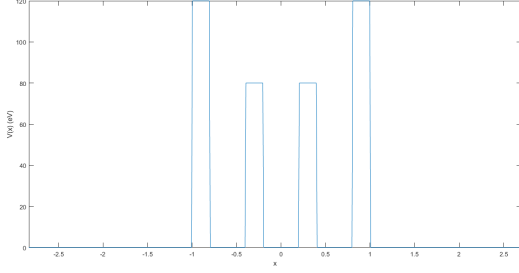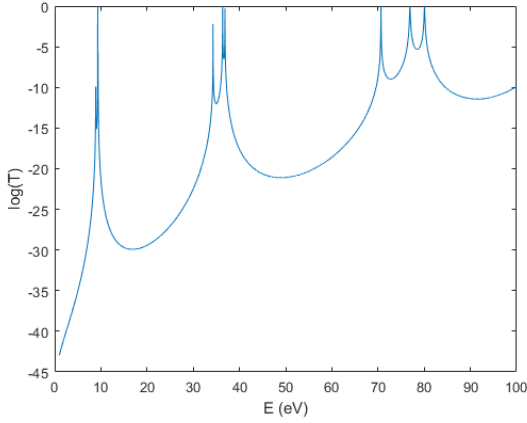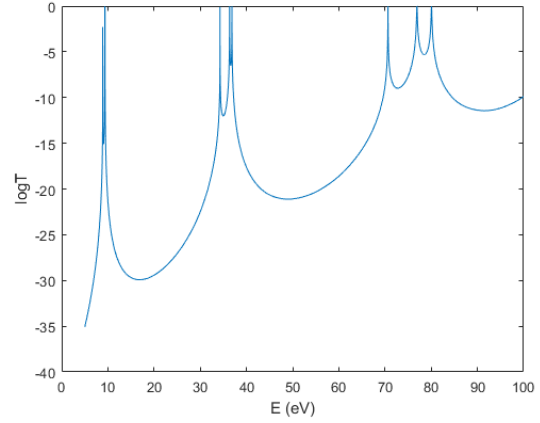

(a) Modified 4 barrier potential (b) Modified 3 barrier potential

Figure 8: Tested modified potentials. On one hand we tried modifying the heights of the intermediate potentials and on the other we increased the weidth of the quantum wells, with 3 barriers.

(a) $log(T)$ for the baseline code (b) $log(T)$ for the optimized code

Figure 9: Test of the optimized code for the modified 4 barriers potential

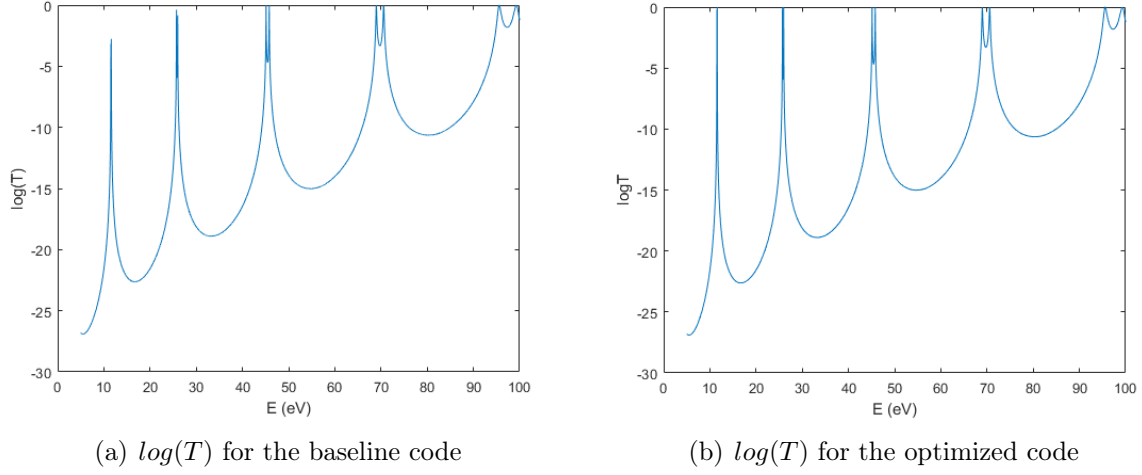(a) $log(T)$ for the baseline code (b) $log(T)$ for the optimized code

Figure 10: Test of the optimized code for the modified 3 barriers potential

From the figures we can appreciate that our optimization passed correctly the presented test, and also we observed that this modifications on the potential produced significant differences on the position of the transmission coefficient's peaks. What's more, from this tests we extracted some remarking features of the model that can be of high interest when building the devices. For instance, we observe that a direct relation between the number of quantum wells and the number of peaks into which the transmission peaks of the 2-barrier is splitted (this effect is better shown in Figure 11). When modifying the height of the intermediate barriers we also observed that the apparent symmetry into which the peaks are splitted is broken, as Figure 9 shows. On the other hand, when increasing the width of the wells, the number of energy states inside the well is also increased, allowing for more resonant transmission peaks. This effect is already shown in Figure 10 and is exaggerated in Figure 12.
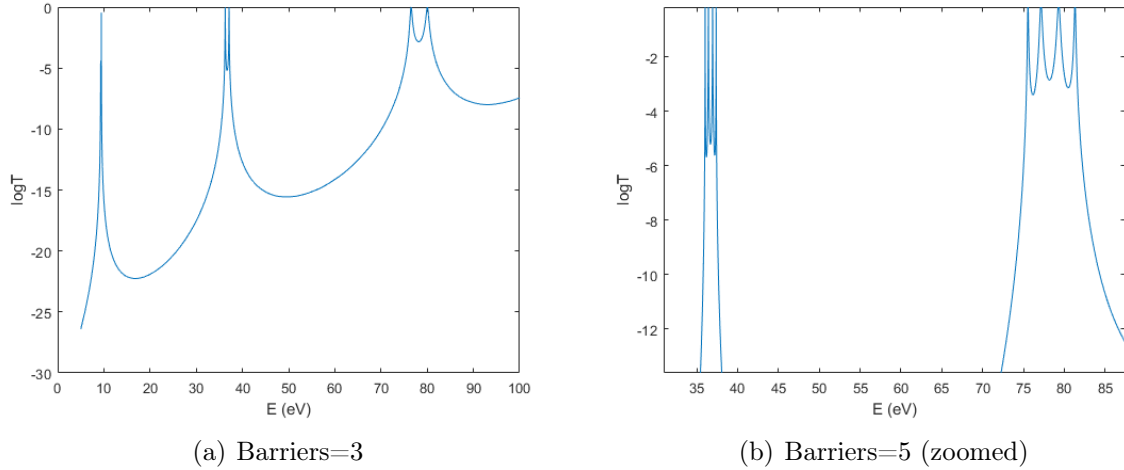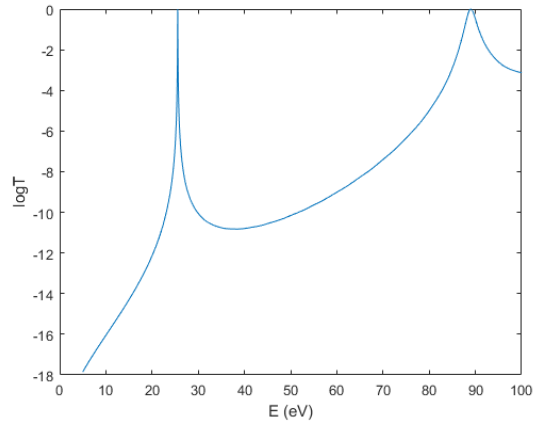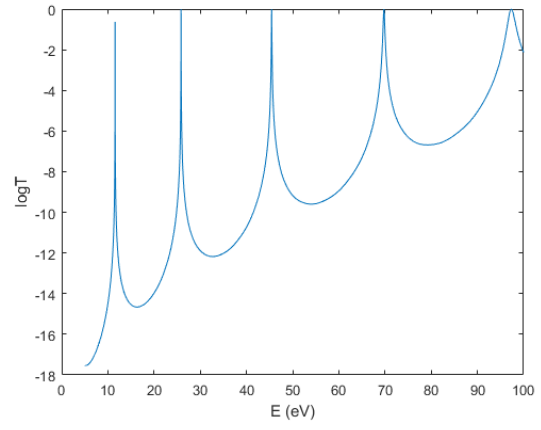

(a) Barriers=3 (b) Barriers=5 (zoomed)

Figure 11: Illustration of how increasing the number of barriers splits the peaks in the same amount.

(a) Well width =0.2   (b) Well width=0.8

Figure 12: Illustration of how increasing the width of the wells allow for more energy resonances.

References

[1] Incident wave definition
https://uk.farnell.com/incident-wave-definition

[2] Transmission coefficient
https://en.wikipedia.org/wiki/Transmission_coefficient

[3] Conservation of probability
https://quantummechanics.ucsd.edu/ph130a/130_notes/node127.html

[4] Probability current
https://en.wikipedia.org/wiki/Probability_current

[5] Stationary state
https://en.wikipedia.org/wiki/Stationary_state